

Dipole transition matrix elements for systems with power-law potentials

Aaron K. Grant and Jonathan L. Rosner

Enrico Fermi Institute and Department of Physics, University of Chicago, Chicago, Illinois 60637

(Received 23 June 1992)

We study the behavior of dipole matrix elements for systems bound by power-law potentials of the form $V(r) \sim r^\alpha$, which are useful in the descriptions of quarkonium systems. The experimental feature for which further understanding is sought is the apparent suppression of the transition $\Upsilon(3S) \rightarrow \chi_b \gamma$. We find that this matrix element actually vanishes in a power-law potential r^α for a certain power $\alpha_0 \approx -0.4$. The suppression of transitions between states with different numbers of nodes in their radial wave functions is a universal property of most physically interesting power-law potentials. We derive results in the limit of large orbital angular momenta l , checking that they agree with the known answers for the Coulomb and spherical oscillator potentials. For states with n_r nodes in their radial wave functions, we find that the matrix elements $\langle n_r, l | r | n_r, l+1 \rangle$ behave as $l^{2/(2+\alpha)}$ for small n_r and large l . Transitions with $\Delta n_r = \pm 1$ behave with respect to those with $\Delta n_r = 0$ as const/\sqrt{l} , with constants calculated for each n_r . Moreover, we find that $\langle n_r=0, l | r | n_r=2, l-1 \rangle / \langle n_r=0, l | r | n_r=0, l+1 \rangle \rightarrow \Phi(\alpha)/l$ as $l \rightarrow \infty$, where $\Phi(\alpha)$ is calculated explicitly.

PACS number(s): 12.40.Qq, 13.20.Gd, 13.40.Hq, 14.40.Gx

I. INTRODUCTION

One of the interesting features of the spectrum of atomic hydrogen is the suppression of transitions where the principal quantum number n and the orbital angular momentum l change in opposite directions relative to those where n and l both increase or both decrease [1,2]. For instance, the radial part of the dipole transition matrix element for a $4d-3p$ transition is 7.6, compared with 1.3 for a $4p-3d$ transition. We see that the transition where n and l change in opposite directions (that is, the $4p-3d$ transition) is roughly 30 times less probable than the transition where n and l both decrease.

Similar features are observed in the spectra of systems bound by non-Coulombic potentials. An example is the system consisting of a b quark and a \bar{b} antiquark, for which the potential is approximately logarithmic ($\alpha \approx 0$) [3]. The spectrum of this system, and the levels predicted by a logarithmic potential, are shown in Fig. 1. Two p -wave levels lie below the $\Upsilon(3S)$ state. The matrix element for the electric dipole transition from the $\Upsilon(3S)$ to the lower fine-structure multiplet of these two levels [the line (a)] is highly suppressed [4] in comparison with that for the transition to the higher fine-structure multiplet [the line (b)]. The transition (c), which involves a change in the number of nodes in the radial wave function, has a smaller matrix element than the transition (d), which does not.

Given the appearance of such spectral features in widely differing systems, it is of interest to ask whether this suppression of certain transitions relative to others is a universal feature of all power-law potentials.

In this paper we compute the radial integrals appearing in the dipole transition matrix elements for a variety of power-law potentials. We are particularly interested in transitions between states having large angular momenta l and whose radial wave functions have only a few nodes,

for this is the case where the suppression of certain transitions is the most dramatic. We find that the degree of suppression is indeed directly dependent on the difference in the number of nodes of the radial wave functions, and estimate this suppression quantitatively for large l . We also find that the transition illustrated by (a) in Fig. 1 vanishes for a specific power $\alpha_0 \approx -0.4$.

The correspondence principle [1] allows one to visualize the favored dipole transitions for large l . An electron in a state of the highest possible l for a given energy has a

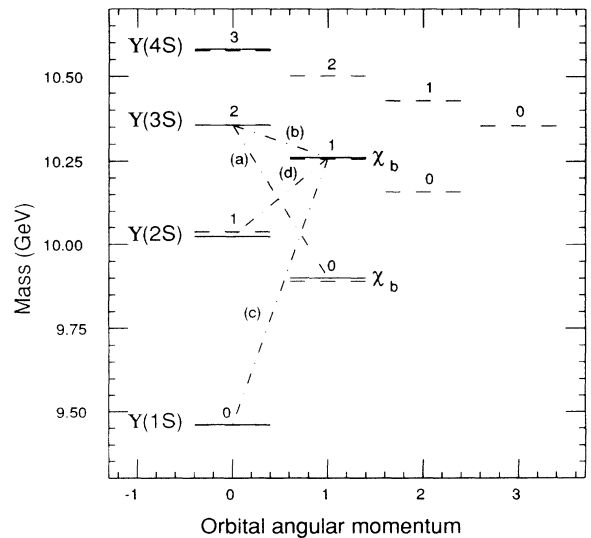


FIG. 1. Spectrum of $b\bar{b}$ bound states. Solid horizontal lines correspond to observed levels; dashed ones correspond to predictions based on a potential $V(r) = \text{const} + 0.72 \text{ GeV} \ln r$. The electric dipole transitions (a), (b), (c), and (d) are discussed in the text. Levels are labeled by the number of nodes of the radial wave function in the interval $0 < r < \infty$.

circular Bohr orbit. Radiation is emitted by loss of angular momentum. Thus, for high l , one should expect transitions with $\Delta l = -1$ for emission and $\Delta l = 1$ for absorption to be favored over those with the opposite signs of Δl . Another argument leading to the same conclusion may be given in terms of WKB wave functions [2].

To provide benchmarks for the general result, we first review the exact results for the Coulomb potential in Sec. II and for the spherical harmonic oscillator in Sec. III. We then give approximate results in Sec. IV, valid for large l , for general power-law potentials having the form $V(r) = r^\alpha/\alpha$, with $-2 < \alpha$. Section V contains a brief discussion of the application of our results to the bound states of heavy quarks, while Sec. VI concludes.

II. COULOMB POTENTIAL

The radial Schrödinger equation for the Coulomb potential, in appropriate units, is

$$-\frac{1}{2} \frac{d^2 u_{\epsilon l}}{dr^2} + \frac{1}{2} \frac{l(l+1)}{r^2} u_{\epsilon l} - \frac{1}{r} u_{\epsilon l} = \epsilon u_{\epsilon l}. \quad (1)$$

Here we are using the rescaled radial wave function $u_{\epsilon l}(r) = rR_{\epsilon l}(r)$. In evaluating the radial dipole integrals, it is convenient to factorize Eq. (1) using the method of Infeld and Hull [5]. This factorization enables us to derive recursion relations for the dipole integrals, which then make their evaluation quite straightforward. We first introduce the raising and lowering operators A_l and A_l^\dagger , defined as

$$A_l = -\frac{d}{dr} + \frac{l+1}{r} - \frac{1}{l+1}, \quad (2)$$

$$A_l^\dagger = \frac{d}{dr} + \frac{l+1}{r} - \frac{1}{l+1},$$

and observe that Eq. (1) may be written in either of the following forms:

$$A_l^\dagger A_l u_{\epsilon l} = \left[2\epsilon + \frac{1}{(l+1)^2} \right] u_{\epsilon l}, \quad (3)$$

or, alternatively,

$$A_{l-1} A_{l-1}^\dagger u_{\epsilon l} = \left[2\epsilon + \frac{1}{l^2} \right] u_{\epsilon l}. \quad (4)$$

To illustrate how A_l and A_l^\dagger can be used as raising and lowering operators, multiply Eq. (3) on the left by A_l . This gives

$$A_l A_l^\dagger (A_l u_{\epsilon l}) = \left[2\epsilon + \frac{1}{(l+1)^2} \right] A_l u_{\epsilon l}. \quad (5)$$

Comparing with Eq. (4) we see that

$$A_l u_{\epsilon l} = \alpha u_{\epsilon l+1}, \quad (6)$$

where α is a normalization constant. A similar argument beginning from Eq. (4) yields

$$A_{l-1}^\dagger u_{\epsilon l} = \beta u_{\epsilon l-1}. \quad (7)$$

In general, of course, it is not possible to raise l an arbitrary

number of times [6]. Rather, there exists a maximum l , l_{\max} , for which

$$A_{l_{\max}} u_{\epsilon l_{\max}} = 0. \quad (8)$$

Equation (8) is significant for two reasons. First, it allows us to determine the energy eigenvalue ϵ : multiplying (8) on the left by $A_{l_{\max}}^\dagger$ and comparing with (3) gives

$$\epsilon = -\frac{1}{2(l_{\max}+1)^2}, \quad l_{\max} = 0, 1, 2, \dots \quad (9)$$

Defining the principal quantum number n by $n = l_{\max} + 1$, we see that (9) gives the usual hydrogenic energies. Equation (8) is also important because it gives us a first-order differential equation for the “key” eigenfunction $u_{\epsilon l_{\max}}$: from (2) we have

$$-\frac{d}{dr} u_{\epsilon l_{\max}} + \frac{l_{\max}+1}{r} u_{\epsilon l_{\max}} - \frac{1}{l_{\max}+1} u_{\epsilon l_{\max}} = 0.$$

The normalized solution to this equation is

$$u_{n l_{\max}} = \frac{1}{\sqrt{(2n)!}} \left[\frac{2}{n} \right]^{n+1/2} r^n e^{-r/n}, \quad (10)$$

where we have replaced the subscript ϵ with the (equivalent) subscript n . (We shall use n in this section to denote the principle quantum number; elsewhere we have used n as a shorthand for n_r , the number of nodes in the radial wave function.) We can now determine the normalization constants α and β appearing in Eqs. (6) and (7). Squaring (6) and integrating over all r gives

$$\begin{aligned} \alpha^2 \int_0^\infty (u_{n, l+1})^2 dr &= \int_0^\infty (A_l u_{nl})^2 dr \\ &= \int_0^\infty u_{nl} A_l^\dagger A_l u_{nl} dr \\ &= \left[-\frac{1}{n^2} + \frac{1}{(l+1)^2} \right] \int_0^\infty u_{nl}^2 dr. \end{aligned}$$

If all the radial wave functions u_{nl} are to be normalized, this implies

$$\alpha = \left[-\frac{1}{n^2} + \frac{1}{(l+1)^2} \right]^{1/2}.$$

A similar argument can be used to determine β . Defining the normalization constants c_{nl} by

$$c_{nl} = \left[\frac{1}{(l+1)^2} - \frac{1}{n^2} \right]^{1/2}, \quad (11)$$

we see that Eqs. (6) and (7) may be rewritten as

$$A_l u_{nl} = c_{nl} u_{n, l+1}, \quad A_{l-1}^\dagger u_{nl} = c_{n, l-1} u_{n, l-1}.$$

We are finally in a position to derive the desired recursion relations. First we observe the identity

$$2l A_{l-1}^\dagger = (2l+1) A_l^\dagger + A_l - \frac{4l+2}{r}. \quad (12)$$

Multiplying this on the left by $r u_{n, l}$ and on the right by u_{nl} and integrating, we obtain, after a little manipulation,

$$2lc_{n,l-1} \int_0^\infty ru_{n'l}u_{n,l-1}dr = (2l+1)c_{n'l} \int_0^\infty ru_{n',l+1}u_{nl}dr + c_{nl} \int_0^\infty ru_{n'l}u_{n,l+1}dr - 3(2l+1) \int_0^\infty u_{n'l}u_{nl}dr . \tag{13}$$

Finally, defining the radial dipole integrals by

$$D_{n'l}^{n'l} = \int_0^\infty ru_{nl}u_{n'l}dr ,$$

we see that (13) may be rewritten as

$$2lc_{n,l-1}D_{n,l-1}^{n'l} = (2l+1)c_{n'l}D_{nl}^{n',l+1} + c_{nl}D_{n,l+1}^{n'l} - 3(2l+1)\delta_{n'n} . \tag{14}$$

We may now apply Eq. (14) to compute radial matrix elements for various transitions. Examples of electric dipole transitions for the Coulomb potential are illustrated in Fig. 2.

We first consider transitions where the principal quantum number changes by one. We may obtain our starting point for the application of the recursion relations by explicitly evaluating the integral at the ‘‘top’’ of the ladder. Using the eigenfunctions given by (10) we have

$$D_{n+1,n}^{n,n-1} = \int_0^\infty ru_{n,n-1}u_{n+1,n}dr = \sqrt{(2n+1)(2n+2)} \frac{2^{2n+2}}{(2n+1)^{2n+3}} (n+1)^{n+3/2} n^{n+5/2} \simeq n^2 . \tag{15}$$

We have given the limiting form, valid for large n . Applying the recursion relation (14) to lower l by one, we find

$$D_{n+1,n-1}^{n,n-2} = \frac{2n-1}{2n-2} \frac{c_{n+1,n-1}}{c_{n,n-2}} D_{n+1,n}^{n,n-1} \simeq \left[1 - \frac{1}{n} \right] D_{n+1,n}^{n,n-1} \simeq n^2 \tag{16}$$

and

$$D_{n+1,n-2}^{n,n-1} = \frac{1}{2n-2} \frac{c_{n+1,n-1}}{c_{n+1,n-2}} D_{n+1,n}^{n,n-1} \simeq \frac{n}{2\sqrt{2}} . \tag{17}$$

By repeatedly lowering l in this manner, it is straightforward to show that similar results hold quite generally for $n \gg 1$ and $l \sim n$: the radial integrals for transitions where n and l change in the same direction scale as n^2 , while those for transitions where n and l change in opposite directions scale as n . In the case of transitions where n and l change in the same direction, the overall coefficient of n^2 is the same as that given in (16); namely, one. In the case of transitions where n increases while l decreases (or vice versa), the overall coefficient of n has a rather

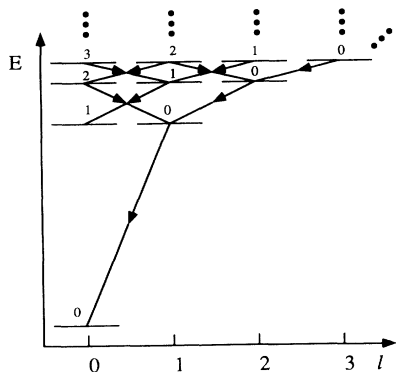


FIG. 2. Spectrum of levels and some electric dipole transitions for a Coulomb potential. Levels are labeled as in Fig. 1.

complicated form, but the leading dependence on n is the same as that given in (17). We therefore find that the ratio of the integrals is

$$\frac{D_{n+1,l-1}^{n,l}}{D_{n+1,l}^{n,l-1}} \propto \frac{1}{l} , \tag{18}$$

for $n \gg 1$ and $n \sim l$. Hence we see that, as n and l increase, the suppression of the ‘‘weak’’ transition becomes more and more pronounced. The results of Eqs. (16) and (17) may be restated in terms of the number of nodes of the radial wave functions: we find that transitions between states having equal numbers of nodes are strongly preferred over transitions between states having k nodes and states having $k \pm 2$ nodes.

We may also compare transitions in which the number of nodes changes by one with those in which the number of nodes does not change.

When the principal quantum number does not change, the number of nodes n_r and the orbital angular momentum l satisfy $\Delta n_r = -\Delta l = \pm 1$ for electric dipole transitions. For the transition from a state with one node to a state with none, direct calculation using the eigenfunction (10) for $u_{n,n-1}$ and the eigenfunction $u_{n,n-2} = A_{n-2}^\dagger u_{n,n-1} / c_{n,n-2}$ yields

$$D_{n,n-1}^{n,n-2} = \int_0^\infty ru_{n,n-1}u_{n,n-2}dr = -3n\sqrt{2n-1}/2 . \tag{19}$$

This expression behaves as $n^{3/2}$ for large n , intermediate between the cases (16) and (17). The change in the number of nodes in the radial wave function here is one; in (16) it is zero, while in (17) it is two.

Equation (19) provides the starting point for a recursive relation allowing calculation of other electric dipole transitions between states of the same n . Taking $n' = n$ in Eq. (14) we find

$$lc_{n,l-1}D_{nl}^{n,l-1} = (l+1)c_{nl}D_{n,l+1}^{n,l} - 3(2l+1)/2 . \tag{20}$$

If we choose $l = n - 3$ in this relation we find from (19) that

$$D_{n,n-2}^{n,n-3} = -3n\sqrt{n-1} . \tag{21}$$

This expression also behaves as $n^{3/2}$ for large n . One can see that the same will be true for any matrix element $D_{nl}^{n',l-1}$ in the limit $n \rightarrow \infty, n-l$ fixed.

Transitions with $\Delta n_r = \Delta l = \pm 1$ involve a change in principal quantum number by two units. An explicit calculation leads to the result

$$D_{n,n-1}^{n+2,n} = \frac{n^{n+(5/2)}(n+2)^{n+2}\sqrt{2n+1}}{2(n+1)^{2n+(7/2)}}, \tag{22}$$

which behaves as $n^{3/2}/\sqrt{2}$ for $n \rightarrow \infty$. Application of the recursion relation (14) for $n'=n+2$ leads to the result

$$D_{n,n-2}^{n+2,n-2} / D_{n,n-1}^{n+2,n} = \sqrt{2n-1}\sqrt{n-1}/(n+2), \tag{23}$$

which tends to $\sqrt{2}$ as $n \rightarrow \infty$. We shall in Sec. IV see that the asymptotic results are part of a more general pattern.

III. SPHERICAL HARMONIC OSCILLATOR

The radial Schrödinger equation for the spherical harmonic oscillator, in appropriate units, is

$$-\frac{1}{2} \frac{d^2 u_{nl}}{dr^2} + \frac{1}{2} \frac{l(l+1)}{r^2} u_{nl} + \frac{1}{2} r^2 u_{nl} = \epsilon_{nl} u_{nl}. \tag{24}$$

The normalized solutions can be written in terms of generalized Laguerre polynomials [8,9] as

$$u_{nl}(r) = \left[\frac{n!}{\Gamma(n+l+3/2)} \right]^{1/2} r^{l+1} L_n^{(l+1/2)}(r^2) e^{-r^2/2}. \tag{25}$$

The corresponding energies are

$$\epsilon_{nl} = 2n + l + \frac{3}{2}, \quad n=0, 1, 2, \dots \tag{26}$$

In this section the quantum number n refers to the number of nodes of the radial wave function. We now wish to compute the radial dipole integrals $D_{nl}^{n',l-1}$ given by

$$D_{nl}^{n',l-1} = \int_0^\infty r u_{nl} u_{n',l-1} dr. \tag{27}$$

These integrals can be readily evaluated if we first make note of the identity [5]

$$L_n^{(l-1/2)}(r^2) = L_n^{(l+1/2)}(r^2) - L_{n-1}^{(l+1/2)}(r^2). \tag{28}$$

Substituting the eigenfunctions (25) into Eq. (27) and using this identity, we find

$$D_{nl}^{n',l-1} = \left[\frac{4n!n'}{\Gamma(n+l+3/2)\Gamma(n'+l+1/2)} \right]^{1/2} \times \int_0^\infty r^{2l+2} L_n^{(l+1/2)}(r^2) \times [L_n^{(l+1/2)}(r^2) - L_{n-1}^{(l+1/2)}(r^2)] e^{-r^2} dr. \tag{29}$$

If we now change variables from r to $x=r^2$ and use the fact that

$$\int_0^\infty x^\alpha L_n^{(\alpha)}(x) L_n^{(\alpha)}(x) e^{-x} dx = \frac{\Gamma(n+\alpha+1)}{n!} \delta_{n'n},$$

we obtain the desired result

$$D_{nl}^{n',l-1} = \sqrt{n+l+\frac{1}{2}} \delta_{nn'} + \sqrt{n+1} \delta_{n,n'-1}. \tag{30}$$

To make the connection with the corresponding results for the Coulomb case, we observe that Eq. (16) refers to transitions between states which both have one node, while (17) refers to transitions between a state having no nodes and a state having two nodes. Hence setting $n=n'=1$ in (30) will give the result corresponding to (16) and setting $n=0, n'=2$ will give the result corresponding to (17). We find

$$D_{1,l}^{1,l-1} = \sqrt{l+\frac{3}{2}} \approx \sqrt{l}, \quad l \gg 1 \tag{31}$$

corresponding to (16), and

$$D_{0,l}^{2,l-1} = 0 \tag{32}$$

corresponding to (17). Hence we find that the transitions described by the latter equation, which are suppressed in the case of the Coulomb potential, are strictly forbidden in the case of the spherical oscillator. Setting $n'=n+1$ in (30) we find that

$$D_{n,l}^{n+1,l-1} = \sqrt{n+1}, \tag{33}$$

corresponding to (19) and (21). The transition matrix elements are not zero, but they do not grow with l . As in the Coulomb case, there is a hierarchy of transition strengths according to the change in the number of nodes of the radial wave function. The allowed electric dipole transitions for a harmonic oscillator are shown in Fig. 3.

A more elementary derivation of the selection rule (32) can be given if we use the factorization of the spherical oscillator Hamiltonian. The full Hamiltonian for the spherical oscillator is

$$H = \frac{1}{2} \mathbf{P}^2 + \frac{1}{2} \mathbf{X}^2. \tag{34}$$

As is well known, this Hamiltonian can be rewritten in terms of raising and lowering operators in the form

$$H = a_x^\dagger a_x + a_y^\dagger a_y + a_z^\dagger a_z + \frac{3}{2}, \tag{35}$$

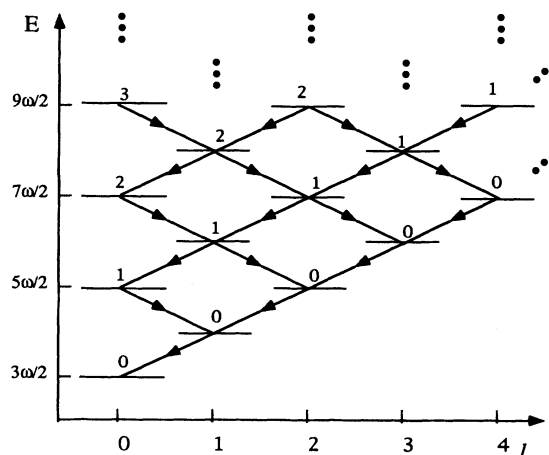


FIG. 3. Spectrum of levels and allowed electric dipole transitions for a harmonic oscillator potential. Levels are labeled as in Fig. 1.

where $a_x = (x + ip_x)/\sqrt{2}$, and similarly for a_y and a_z . The eigenstates of this Hamiltonian are the usual Fock states $|n_1, n_2, n_3\rangle$, which satisfy

$$H|n_1, n_2, n_3\rangle = (n_1 + n_2 + n_3 + \frac{3}{2})|n_1, n_2, n_3\rangle. \quad (36)$$

If we now introduce a dipole interaction term of the form $V(t) = E_0 z e^{-i\omega t}$, corresponding to a linearly polarized electromagnetic wave, we see that the relevant dipole transition matrix elements have the form

$$D_{m_1 m_2 m_3}^{n_1 n_2 n_3} = \langle n_1, n_2, n_3 | z | m_1, m_2, m_3 \rangle. \quad (37)$$

For simplicity we have chosen the polarization of the incident wave along the z axis, but this clearly involves no loss of generality. To evaluate these matrix elements we first observe that z may be written as

$$z = \frac{a_z + a_z^\dagger}{\sqrt{2}}. \quad (38)$$

Furthermore, the action of the raising and lowering operators on the basis kets is given by

$$a_z |n_1, n_2, n_3\rangle = \sqrt{n_3} |n_1, n_2, n_3 - 1\rangle \quad (39)$$

and

$$a_z^\dagger |n_1, n_2, n_3\rangle = \sqrt{n_3 + 1} |n_1, n_2, n_3 + 1\rangle. \quad (40)$$

Using these results to evaluate $D_{m_1 m_2 m_3}^{n_1 n_2 n_3}$ gives

$$D_{m_1 m_2 m_3}^{n_1 n_2 n_3} = \delta_{n_1 m_1} \delta_{n_2 m_2} \left[\left[\frac{m_3}{2} \right]^{1/2} \delta_{n_3, m_3 - 1} + \left[\frac{m_3 + 1}{2} \right]^{1/2} \delta_{n_3, m_3 + 1} \right]. \quad (41)$$

From this we see that the allowed transitions are those that take place between states whose energies differ by one; all other transitions are strictly forbidden. This selection rule is in fact equivalent to the selection rule given by Eq. (30): since the states $u_{0,l}$ and $u_{2,l-1}$ have energies which differ by two, dipole transitions between these states are forbidden.

IV. GENERAL POWER-LAW POTENTIALS

In this section we consider the radial Schrödinger equation for a general power-law potential:

$$\left[-\frac{1}{2} \frac{d^2}{dr^2} + U_\pm(r) \right] u_{nl} = \epsilon_{nl} u_{nl}, \quad (42)$$

where the problem with orbital angular momentum l corresponds to the effective potential $U_+(r)$ given by

$$U_+(r) = \frac{1}{2} \frac{l(l+1)}{r^2} + \frac{1}{\alpha} r^\alpha, \quad (43)$$

and the one with orbital angular momentum $l-1$ corresponds to

$$U_-(r) = \frac{1}{2} \frac{l(l-1)}{r^2} + \frac{1}{\alpha} r^\alpha. \quad (44)$$

In general, it is not possible to give exact analytical solutions to these equations. For very large l , however, we may construct approximate solutions by expanding $U_\pm(r)$ about the average of their minima:

$$\bar{r}_l = l^{2/(2+\alpha)}. \quad (45)$$

This method has been applied elsewhere [10,11] to the large- l behavior of other problems. Equation (42) then reduces to the Schrödinger equation for a shifted one-dimensional harmonic oscillator, with perturbing terms. Approximate solutions can then be given in terms of a perturbation expansion. The corresponding unperturbed energies are given by the familiar formula $\epsilon_n = (n + 1/2)\omega$, where ω is the oscillator frequency.

Explicitly, we may write

$$U_\pm(r) = \frac{1}{2} \omega^2 x^2 + \sum_{j=1}^4 c_j^\pm x^j + \dots, \quad (46)$$

where $x \equiv r - \bar{r}$, and the coefficients for $j > 4$ will not be needed. The parameters ω^2, c_j^\pm are

$$\omega^2 = (2 + \alpha) l^{2(\alpha-2)/(\alpha+2)} \quad (47)$$

and

$$c_1^\pm = \mp l^{(\alpha-4)/(\alpha+2)}, \quad (48)$$

$$c_2^\pm = \pm \frac{3}{2} l^{(\alpha-6)/(\alpha+2)}, \quad (49)$$

$$c_3^\pm = l^{2(\alpha-3)/(\alpha+2)} \left[\frac{\alpha^2 - 3\alpha - 10}{6} \mp \frac{2}{l} \right], \quad (50)$$

$$c_4^\pm = l^{2(\alpha-4)/(\alpha+2)} \left[\frac{(\alpha-1)(\alpha-2)(\alpha-3)}{24} + \frac{5}{2} \left[1 \pm \frac{1}{l} \right] \right]. \quad (51)$$

The corresponding Hamiltonians have the form

$$H_\pm = H_0 + \sum_{j=1}^4 c_j^\pm x^j + \dots \quad (52)$$

with

$$H_0 \equiv (a^\dagger a + \frac{1}{2})\omega, \quad a \equiv \left[\frac{\omega}{2} \right]^{1/2} \left[x + i \frac{p}{\omega} \right]. \quad (53)$$

The zero-order states are Fock states $|k\rangle$; we have

$$\begin{aligned} H_0 |k\rangle &= (k + \frac{1}{2})\omega |k\rangle, \\ a |k\rangle &= \sqrt{k} |k-1\rangle, \\ a^\dagger |k\rangle &= \sqrt{k+1} |k+1\rangle. \end{aligned} \quad (54)$$

The perturbing Hamiltonians can be written in terms of a and a^\dagger using $x = (a + a^\dagger)/(2\omega)^{1/2}$.

Notice that ω is real, according to (47), only for $2 < \alpha$. It is only in such a case that the effective potential has a minimum at $r = \bar{r}_l$. Otherwise, the point at which its first derivative vanishes actually is a local *maximum*.

The leading matrix elements will be those which in-

volve an expectation value of the quantity \bar{r} between unperturbed states. Thus, for any finite number of nodes n_r of the radial wave functions, as long as our oscillator expansion is valid, we can conclude that

$$\langle n_r, l-1 | r | n_r, l \rangle \approx \bar{r} = l^{2/(2+\alpha)}. \quad (55)$$

We next calculate matrix elements for which the number of nodes of the radial wave function changes by 1. We shall be concerned with the transitions $|n_r, l-1\rangle \rightarrow |n_r-1, l\rangle$ and $|n_r-1, l-1\rangle \rightarrow |n_r, l\rangle$. We shall drop the subscript r on n in what follows.

One contribution to such matrix elements will come from the term x in $r = \bar{r} + x$, since x connects unperturbed states $|k\rangle$ differing in k by 1. However, another set of contributions comes from the expansion of the states in the presence of the perturbing terms in the potentials (46). Denoting the unperturbed states by labels without l , we may write

$$\begin{aligned} |n, l-1\rangle = & |n\rangle + c_1^- \frac{|n-1\rangle \langle n-1 | x | n \rangle}{\omega} \\ & + c_3^- \frac{|n-1\rangle \langle n-1 | x^3 | n \rangle}{\omega}, \end{aligned} \quad (56)$$

$$\begin{aligned} |n-1, l\rangle = & |n-1\rangle + c_1^+ \frac{|n\rangle \langle n | x | n-1 \rangle}{-\omega} \\ & + c_3^+ \frac{|n\rangle \langle n | x^3 | n-1 \rangle}{-\omega}, \end{aligned} \quad (57)$$

$$\begin{aligned} |n, l\rangle = & |n\rangle + c_1^+ \frac{|n-1\rangle \langle n-1 | x | n \rangle}{\omega} \\ & + c_3^+ \frac{|n-1\rangle \langle n-1 | x^3 | n \rangle}{\omega}, \end{aligned} \quad (58)$$

$$\begin{aligned} |n-1, l-1\rangle = & |n-1\rangle + c_1^- \frac{|n\rangle \langle n | x | n-1 \rangle}{-\omega} \\ & + c_3^- \frac{|n\rangle \langle n | x^3 | n-1 \rangle}{-\omega}, \end{aligned} \quad (59)$$

where we have retained all terms which can contribute to the matrix element to order $1/\sqrt{l}$ in the large- l limit. Since the leading-order terms in c_3^+ and c_3^- are equal [see Eq. (50)], one finds that these terms cancel in the final result, so that only the perturbations in $U_{\pm}(r)$ linear in x need be taken into account.

Taking account of the relation $c_1^- = -c_1^+$, we find in the limit of large l that

$$\langle n-1, l | r | n, l-1 \rangle \approx \frac{2c_1^- \bar{r}}{\omega} \left[\frac{n}{2\omega} \right]^{1/2} + \langle n-1 | x | n \rangle \quad (60)$$

and

$$\langle n-1, l-1 | r | n, l \rangle \approx \frac{2c_1^+ \bar{r}}{\omega} \left[\frac{n}{2\omega} \right]^{1/2} + \langle n-1 | x | n \rangle. \quad (61)$$

Bearing in mind the expressions for ω and c_1^{\pm} , we find

$$\langle n-1, l | r | n, l-1 \rangle \approx \sqrt{n} \Psi_+(\alpha) l^{(1-[\alpha/2])/(2+\alpha)} \quad (62)$$

and

$$\langle n-1, l-1 | r | n, l \rangle \approx \sqrt{n} \Psi_-(\alpha) l^{(1-[\alpha/2])/(2+\alpha)}, \quad (63)$$

where

$$\Psi_{\pm} = \frac{1}{2^{1/2}(2+\alpha)^{1/4}} \left[1 \pm \frac{2}{(2+\alpha)^{1/2}} \right]. \quad (64)$$

The results (62)–(64) agree with special cases discussed previously. Since

$$\Psi_+(-1) = 3/\sqrt{2}, \quad \Psi_-(-1) = -1/\sqrt{2}, \quad (65)$$

we obtain results corresponding to Eqs. (19) and (21)–(23) for the Coulomb potential. Since

$$\Psi_+(2) = 1, \quad \Psi_-(2) = 0, \quad (66)$$

we find results corresponding to (30) for the harmonic oscillator.

The result when the number n of nodes in the radial wave function changes by two is considerably more involved. For the general $n \rightarrow n-2$ transition, one must expand the states in terms of unperturbed states ranging from $|n-3\rangle$ to $|n+1\rangle$. One is interested in contributions of order $1/l$ with respect to the leading behavior $\bar{r} = l^{2/(2+\alpha)}$. Five such contributions are proportional to $\bar{r} \langle m | m \rangle$, $n-3 \leq m \leq n+1$, while four involve matrix elements of x between states differing in n by 1.

For purposes of illustration, and because it is relevant to the most highly suppressed transition illustrated in Fig. 1 [the line (a)], we calculate the matrix element for the transition $|2, l-1\rangle \rightarrow |0, l\rangle$.

In principle, we need terms in the potentials $U_{\pm}(r)$ up to order x^4 . It turns out that the contributions of c_4^+ and c_4^- to the term of interest cancel, so that in fact only terms up to order x^3 are important. Each state is expanded in terms of unperturbed Fock space states $|m\rangle$, $0 \leq m \leq 3$. The expansions are

$$|0, l\rangle = |0\rangle + a_1^+ |1\rangle + a_2^+ |2\rangle + a_3^+ |3\rangle, \quad (67)$$

$$|2, l-1\rangle = a_0^- |0\rangle + a_1^- |1\rangle + |2\rangle + a_3^- |3\rangle. \quad (68)$$

The coefficients are of the order

$$a_0^-, a_2^+ \sim 1/l, \quad a_{1,3}^{\pm} \sim 1/\sqrt{l}. \quad (69)$$

In order to calculate the terms of order $1/l$ correctly, one has to go up to second order in perturbation theory. Explicitly, the coefficients a_i^{\pm} are expressed in terms of the coefficients c_i^{\pm} as

$$a_1^+ = -\frac{1}{\sqrt{2}\omega^{3/2}} \left[c_1^+ + \frac{3}{2\omega} c_3^+ \right], \quad (70a)$$

$$a_2^+ = \frac{1}{\sqrt{2}\omega^2} \left[-\frac{1}{2}c_2^+ - \frac{3}{2\omega}c_4^+ + \frac{1}{2\omega}(c_1^+)^2 + \frac{5}{2\omega^2}c_1^+c_3^+ + \frac{27}{8\omega^3}(c_3^+)^2 \right], \quad (70b)$$

$$a_3^+ = -\frac{1}{2\sqrt{3}\omega^{5/2}} c_3^+, \quad (70c)$$

$$a_0^- = \frac{1}{2\sqrt{2}\omega^2} \left[c_2^- + \frac{3}{\omega}c_4^- + \frac{1}{\omega}(c_1^-)^2 + \frac{3}{\omega^2}c_1^-c_3^- - \frac{9}{4\omega^3}(c_3^-)^2 \right], \quad (71a)$$

$$a_1^- = \frac{1}{\omega^{3/2}} \left[c_1^- + \frac{3}{\omega}c_3^- \right], \quad (71b)$$

$$a_3^- = -\frac{\sqrt{6}}{2\omega^{3/2}} \left[c_1^- + \frac{9}{2\omega}c_3^- \right]. \quad (71c)$$

Defining

$$f(\alpha) \equiv \frac{1}{6}(\alpha^2 - 3\alpha - 10), \quad (72)$$

$$g(\alpha) \equiv \frac{1}{24}[(\alpha-1)(\alpha-2)(\alpha-3) + 60],$$

$$h(\alpha) \equiv \sqrt{\alpha+2},$$

and using the results (47)–(51) for ω and the c_i^\pm , we find

$$a_1^+ = \frac{1}{\sqrt{2}h^{3/2}} \left[\frac{2h-3f}{2h} \right] l^{-1/2}, \quad (73a)$$

$$a_2^+ = \frac{1}{\sqrt{2}h^2} \left[\frac{-6h^3 - 12gh^2 + 4h^2 - 20fh + 27f^2}{8h^3} \right] l^{-1}, \quad (73b)$$

$$a_3^+ = -\frac{1}{2\sqrt{3}h^{5/2}} f l^{-1/2}, \quad (73c)$$

$$a_0^- = \frac{1}{\sqrt{2}h^2} \left[\frac{-6h^3 + 12gh^2 + 4h^2 + 12fh - 9f^2}{8h^3} \right] l^{-1}, \quad (74a)$$

$$a_1^- = \left[\frac{h+3f}{h^{5/2}} \right] l^{-1/2}, \quad (74b)$$

$$a_3^- = -\frac{\sqrt{6}(2h+9f)}{4h^{5/2}} l^{-1/2}. \quad (74c)$$

The matrix element is

$$\begin{aligned} D_{2,l-1}^{0l} &\equiv \langle 2, l-1 | r | 0, l \rangle \\ &= \bar{r} \langle 2, l-1 | 0, l \rangle + \langle 2, l-1 | x | 0, l \rangle \\ &= \bar{r}(a_0^- + a_2^+ + a_1^+ a_1^- + a_3^+ a_3^- + \dots) \\ &\quad + (2\omega)^{-1/2} (a_1^- + \sqrt{2}a_1^+ + \sqrt{3}a_3^+ + \dots), \end{aligned} \quad (75)$$

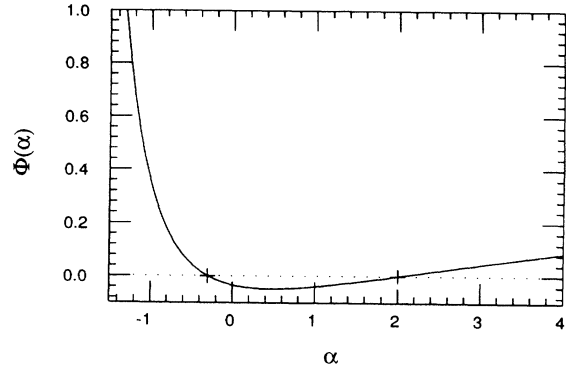


FIG. 4. Function $\Phi(\alpha)$ [Eq. (77)] describing the ratio of electric dipole transitions for potentials $V(r) \sim r^\alpha$. The two zeros of $\Phi(\alpha)$, denoted by the crosses, occur at $\alpha \approx -0.3$ and $\alpha = 2$.

where the ellipses denote states that do not contribute to the order of interest in the limit of large l . The final result is

$$D_{2,l-1}^{0l} = \Phi(\alpha) l^{-\alpha/(2+\alpha)}, \quad (76)$$

where

$$\Phi(\alpha) \equiv \frac{(\alpha-2)[1+(\alpha-1)/(\alpha+2)^{1/2}]}{6\sqrt{2}(\alpha+2)}. \quad (77)$$

The matrix element (76) behaves as $\Phi(\alpha)/l$ with respect to the leading ones (with no change in the number of nodes).

The function $\Phi(\alpha)$ is shown in Fig. 4. It vanishes when $\alpha=2$, in accord with the selection rules noted at the end of Sec. III. It also has a root at $\alpha=(3-\sqrt{13})/2 \approx -0.3$, and is quite small over the range $-1 \leq \alpha \leq 2$. Thus, the suppression of the dipole matrix element $D_{2,l-1}^{0l}$ in the large- l limit is quite a general feature of power-law potentials.

V. APPLICATION TO QUARKONIUM

Let us return to the electromagnetic transitions in the $b\bar{b}$ system, discussed briefly in the Introduction and depicted in Fig. 1. We are now in a position to understand the relative strengths of the electric dipole transitions labeled by (a), (b), (c), and (d). We can do so by comparison with the cases of the Coulomb and harmonic oscillator potentials, and by reference to our general result for power-law potentials in the limit of large l .

The transition (a) is one in which the number of nodes in the radial wave function changes from 2 to 0. We have found that such transitions are highly suppressed in the case of the Coulomb potential, totally absent for the harmonic oscillator, and suppressed by a factor of $\Phi(\alpha)/l$ with respect to the dominant ($n_r=0 \rightarrow n_r=0$) transitions for high l in a power-law potential. The function $\Phi(\alpha)$, shown in Fig. 4, is very small for a wide range of α and vanishes at $\alpha \approx -0.3$ and $\alpha = 2$.

The transition (b) is one in which the number of nodes changes from 2 to 1. This transition is less suppressed than the one just mentioned. In a power-law potential, its strength is suppressed by a factor of const/\sqrt{l} with

respect to the dominant one for high l . The corresponding suppression factor for $n_r=1 \rightarrow n_r=0$ transitions found in Sec. IV is $\Psi_+(r)/\sqrt{l}$, where $\Psi_+(r)$ is the function defined in Eq. (64).

The transition (c) involves a change in the number of nodes (1 the initial and 0 in the final state). This transition is expected to be suppressed in comparison with (d), which involves no change in the number of nodes.

We summarize the Coulomb and harmonic oscillator results for the ratios of dipole matrix elements (a)/(b) and (c)/(d) in Table I. Also shown are the matrix elements as calculated for the logarithmic potential [12]. The ratios are shown as functions of the power α in Fig. 5.

In order to compare the predictions of Table I with experiments, we must extract ratios of dipole matrix elements from experimentally determined branching ratios or decay widths. The information contained in Refs. [4] and [13] allows us to do this. The partial widths for the dipole transitions of interest are given in terms of the matrix elements $\langle r \rangle$ by

$$\frac{4}{3}e_Q^2\alpha\bar{E}_\gamma^3C_f\langle r \rangle_a^2\left\{\frac{2}{9}B[\chi_{b2}\rightarrow\Upsilon(1S)\gamma]+\frac{1}{3}B[\chi_{b1}\rightarrow\Upsilon(1S)\gamma]+\frac{1}{9}B[\chi_{b0}\rightarrow\Upsilon(1S)\gamma]\right\}=(1.7\pm 0.4\pm 0.6)\times 10^{-3}\Gamma_{\text{tot}}[\Upsilon(3S)], \quad (80)$$

where $\bar{E}_\gamma=445$ MeV is the average photon energy for $\Upsilon(3S)\rightarrow\chi_{bj}\gamma$ transitions. We use the result quoted in Ref. [4], $\Gamma_{\text{tot}}[\Upsilon(3S)]=(24.3\pm 2.9)$ keV, and the branching ratios [13] $B[\chi_{b2}\rightarrow\Upsilon(1S)\gamma]=(22\pm 4)\%$, $B[\chi_{b1}\rightarrow\Upsilon(1S)\gamma]=(35\pm 8)\%$, $B[\chi_{b0}\rightarrow\Upsilon(1S)\gamma]<6\%$ (so we neglect this last quantity). We then find

$$|\langle r \rangle_a|=(0.043\pm 0.010) \text{ GeV}^{-1}, \quad (81)$$

leading to the ratio quoted in Table I.

The corresponding calculation for the ratio of the matrix elements (c) and (d) proceeds from the information [4] that

$$\sum_J B[\Upsilon(3S)\rightarrow\chi'_{bJ}\gamma]B[\chi'_{bJ}\rightarrow\Upsilon(2S)\gamma]=(4.2\pm 0.6\pm 0.5)\% \quad (82)$$

with an average photon energy in the second transition of (236.1 ± 2.6) MeV, while

$$\sum_J B[\Upsilon(3S)\rightarrow\chi'_{bJ}\gamma]B[\chi'_{bJ}\rightarrow\Upsilon(1S)\gamma]=(2.0\pm 0.2\pm 0.2)\% \quad (83)$$

with an average photon energy in the second transition of

TABLE I. Predicted ratios of dipole matrix elements in various potentials for transitions shown in Fig. 1, and experimental values.

Ratio	Coulomb ($\alpha=-1$)	Logarithmic ($\alpha=0$)	Oscillator ($\alpha=2$)	Expt. (magnitude)
(a)/(b)	-0.074	0.016	0	0.016 ± 0.004
(c)/(d)	0.168	0.101	0	0.117 ± 0.014

$$\Gamma=\frac{4}{3}e_Q^2\alpha E_\gamma^3 C_f \langle r \rangle^2, \quad (78)$$

where $e_Q=-\frac{1}{3}$ is the charge of the b quark, E_γ is the photon energy, and $C_f=(2J_f+1)/9$ for $S\rightarrow P$, $C_f=\frac{1}{3}$ for $P\rightarrow S$ transitions.

Using the partial widths and photon energies quoted by the CUSB Collaboration [4], we obtain for transition (b) the dipole matrix elements $|\langle r \rangle_b|=(2.59\pm 0.19, 2.78\pm 0.20, 2.63\pm 0.15) \text{ GeV}^{-1}$ for the $J=(0,1,2)$ members of the fine-structure multiplet. These are consistent with one another; their average is

$$|\langle r \rangle_b|=(2.66\pm 0.10) \text{ GeV}^{-1}. \quad (79)$$

The CUSB Collaboration [4] quotes a product of branching ratios for the transitions (a) (summed over fine-structure multiplets) followed by transitions to the $\Upsilon(1S)$. We may interpret this information as providing the combination

(770.3 ± 2.9) MeV. We then find

$$\frac{|\langle r \rangle_c|}{|\langle r \rangle_d|}=\left[\frac{(2.0\pm 0.2\pm 0.2)/(770.3)^3}{(4.2\pm 0.6\pm 0.5)/(236.1)^3}\right]^{1/2} = 0.117\pm 0.014. \quad (84)$$

Notice the change in sign of the ratio (a)/(b) in Table I between $\alpha=-1$ and $\alpha=0$. This ratio actually vanishes at a power $\alpha_0\approx -0.4$, as illustrated in Fig. 5. The experi-

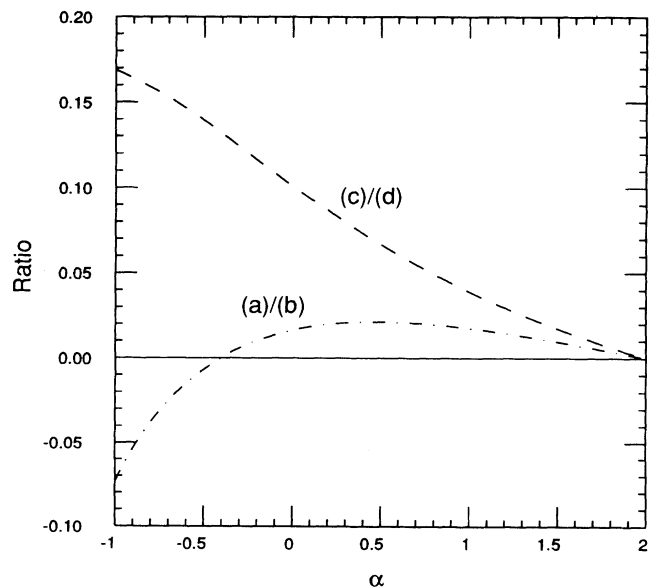


FIG. 5. Ratios of dipole matrix elements in potentials $V(r)\sim r^\alpha$ for transitions shown in Fig. 1.

mental ratio (a)/(b) is compatible at the 1σ level with a range of powers between -0.1 and 0.2 . The ratio (c)/(d) is compatible with any power between 0 and -0.4 . The suppression of these ratios, as we have seen, is an example of a much more general result.

VI. SUMMARY

We have presented both exact and approximate results for the radial dipole integrals for a variety of power-law potentials having the form r^α/α for $-2 < \alpha$. In all cases, we have found that dipole transitions between states whose radial wave functions have the same number of nodes are favored over transitions between states having different numbers of nodes. The larger the difference in number of nodes, the greater the suppression. Transitions with changes in the number of nodes by greater than one are strictly forbidden in the case of the spherical

harmonic oscillator, and thus are suppressed in cases resembling the oscillator [14]. The suppression of these transitions indeed is found to be a universal property of all power law potentials.

Note added. It has been shown [15] that the dipole matrix element between the $2S$ and $1P$ levels of a two-body system [e.g., between $\Upsilon(2S)$ and χ_b in Fig. 1] cannot vanish, and has the sign of the product of the reduced radial wave functions for the two levels as $r \rightarrow \infty$. We thank André Martin for informing us of this result.

ACKNOWLEDGMENTS

We are grateful to Ugo Fano for encouragement and for helpful discussions. This work was supported in part by the United States Department of Energy through Grant No. DE FG02 90ER 40560.

-
- [1] H. Bethe and E. E. Salpeter, *Quantum Mechanics of One- and Two-Electron Atoms* (Academic, New York, 1957), pp. 258 and 259; M. Born, *Atomic Physics*, 7th ed. (Hafner, New York, 1963), pp. 150–154; U. Fano and J. W. Cooper, *Rev. Mod. Phys.* **40**, 441 (1968).
- [2] U. Fano, *Phys. Rev. A* **32**, 617 (1985).
- [3] M. Machacek and Y. Tomozawa, *Ann. Phys. (N.Y.)* **110**, 407 (1978); C. Quigg and Jonathan L. Rosner, *Phys. Lett.* **71B**, 153 (1977); A. Martin, *ibid.* **93B**, 338 (1980).
- [4] CUSB Collaboration, M. Narain *et al.*, *Phys. Rev. Lett.* **67**, 1696 (1991), and references therein. [See also U. Heintz *et al.*, *Phys. Rev. D* **46**, 1928 (1992).] Transitions to the upper set of p -wave levels have also been studied by the CLEO-II Collaboration, R. Morrison *et al.*, *Phys. Rev. Lett.* **67**, 1696 (1991).
- [5] L. Infeld and T. E. Hull, *Rev. Mod. Phys.* **23**, 21 (1951). For a recent application of this method to the Coulomb problem, see O. L. de Lange and R. E. Raab, *Phys. Rev. A* **35**, 951 (1987).
- [6] The proof is straightforward but lengthy. For a detailed proof, see Infeld and Hull [5].
- [7] I. I. Gol'dman and V. D. Krivchenkov, *Problems in Quantum Mechanics* (Addison-Wesley, Reading, MA, 1961), pp. 131 and 132.
- [8] Reference [7] gives a solution in terms of confluent hypergeometric functions. This may be converted to generalized Laguerre polynomials using *Handbook of Mathematical Functions*, edited by M. Abramowitz and I. E. Stegun (Dover, New York, 1972), Eq. 22.5.54.
- [9] *Handbook of Mathematical Functions* [8], Eq. 22.7.30.
- [10] G. Tiktopoulos and S. B. Treiman, *Phys. Rev.* **135**, B711 (1964); **137**, B1597 (1965).
- [11] S.-J. Chang and J. L. Rosner, *Phys. Rev. D* **8**, 450 (1973).
- [12] T. Sterling, *Nucl. Phys.* **B141**, 272 (1978); **B148**, 538(E) (1979). We have corrected some small discrepancies with respect to the values quoted there for the matrix elements corresponding to the suppressed transitions (a) and (c).
- [13] Particle Data Group, J. J. Hernández *et al.*, *Phys. Lett. B* **239**, 1 (1990).
- [14] R. S. Berry, *J. Chem. Phys.* **45**, 1228 (1966).
- [15] A. Martin, in *Proceedings of the Second International Symposium on Hadron Structure and Multiparticle Production*, Kazimierz, Poland, 1979, edited by Z. Ajduk (Institute of Theoretical Physics, Warsaw, 1979), p. 291.